Proceedings of NHTC'00
34th National Heat Transfer Conference
Pittsburgh, Pennsylvania, August 20-22, 2000

NHTC2000-12132

EVALUATION OF THE NANOSCALE HEAT AND MASS TRANSFER MODEL OF LII: PREDICTION OF THE EXCITATION INTENSITY

D. R. Snelling, F. Liu, G. J. Smallwood, and Ö. L. Gülder

Combustion Research Group
Institute for Chemical Process & Environmental Technology
National Research Council Canada
Montreal Road, Ottawa, Ontario, Canada K1A 0R6

ABSTRACT

The current mathematical model developed for the heat and mass transfer processes of laser-induced incandescence (LII) was evaluated in terms of the excitation profile, which relates the prompt LII signal to the laser fluence. The model prediction for the excitation profile is compared with experimental data for both uniform and Gaussian spatial laser intensity distributions. Use of E(m) based on the accepted soot refractive index established by Dalzell and Sarofim for calculation of laser energy absorption by soot results in a much sharper rise of the excitation profile compared to the experimental data. Better overall agreement between the predicted excitation curve and the experimental one was obtained by using the value of E(m) based on the soot refractive index established by Lee and Tien. The predicted excitation profile of the prompt LII signal is more sensitive to uncertainties in the value of E(m) than to the initial particle size and the detection gate width and timing. The temporal profile of the pulsed laser intensity has a much less effect on the excitation curve than the spatial profile of the laser but significantly affects the history of soot temperature and diameter.

INTRODUCTION

Laser-induced incandescence (LII) has emerged as a powerful diagnostic technique for spatially and temporally resolved measurements of soot volume fraction and primary particle size. In this technique, the soot particles in the measurement volume are heated up rapidly from the local combustion gas temperature to above the soot vaporization temperature (about 4000 K) using a pulsed laser with duration typically below 20 ns FWHM. With proper calibration, analysis of the incandescence signal from the heated soot particles yields information on the local soot volume fraction and primary particle size. The absorption of laser energy by soot particles and the subsequent cooling processes involve nano-scale heat and mass transfer in both time and space. Development of the mathematical model describing the heat and mass transfer processes of LII is of importance to understand and interpret the experimental results and to facilitate the improvement and further application of this technique, especially for measurement of primary soot particle size.

In addition to its high temporal and spatial resolution, another important feature of LII technique is its weak dependence on laser energy once a threshold value is reached (Shaddix and Smyth, 1996). Extensive experimental studies on the variation of the prompt LII signal (time-integrated signal near the peak signal over a short period of time typically around 10 ns) with laser intensity have been carried out (Tait and Greenhalgh, 1993; Vander Wal and Weiland, 1994; Ni et al., 1995; Shaddix and Smyth, 1996; Snelling et al., 1997; Vander Wal and Jensen, 1998; Wainner and Seitzman, 1999). The dependence of the LII signal on laser fluence is often referred to as the *excitation curve* in the literature. Most of these experiments showed that as the laser fluence increases the LII signal first rises very rapidly to reach a near plateau then it either gradually increases or decreases, depending on the spatial profile of the pulsed laser beam (Ni et al., 1995; Tait and Greenhalgh, 1993). It is worth noting that most of these experiments investigated the excitation curve using laser fluences less than about 1 J/cm^2. At higher laser fluences (above 1 J/cm^2), Wainner and Seitzman (1999) showed that the LII signal increases monotonically with increasing laser fluence. The LII signal at high laser fluences may contain significant emission from the C_2 swan bands in addition to the thermal radiation of soot. While the fluence dependence of the LII signal has been extensively studied experimentally, only few

studies made attempts to model the experimentally observed excitation curve (Tait and Greenhalgh, 1992, 1993; Snelling et al., 1997). Tait and Greenhalgh (1992, 1993) modelled the excitation curve of a 100 nm soot particle heated by a pulsed laser at 308 nm and 1064 nm. They also investigated the effects of the laser beam spatial profile (rectangular and Gaussian). Reasonably good agreement between the experimental and the modelled excitation curves was observed with the measurement taken in a turbulent propane flame where the soot particle size was not known (Tait and Greenhalgh, 1993). In addition, they reported the LII signal variation with 'laser fluence' in W/cm^2. Shaddix and Smyth (1996) suggested that the laser fluence (J/cm^2) should be reported for the laser power dependence of LII signal instead of the laser intensity (W/cm^2). Snelling et al. (1997) make an attempt to predict the laser fluence dependence of LII signal from a laminar ethylene flame where the primary soot particle size was well documented. A Gaussian-shaped laser beam was used in their experimental work and the proper treatment of the non-uniform laser intensity distribution across the laser beam was incorporated into their modelling. Their predicted excitation curves (prompt and integrated), however, do not reproduce the experimentally observed laser fluence dependence of LII signal. Their predicted LII signals increase monotonically with increasing laser fluence while the experimental curves first increase with increasing laser fluence to a maximum then decrease at higher laser fluences.

Compared to experimental research of LII, less effort has been devoted to the development of theoretical LII model due to many complexities involved in the heat and mass transfer processes of pulsed laser heating of soot particles. First, an accurate value of E(m) of soot is required in order to reliably calculate the laser energy absorption by soot particles. However, there are considerable uncertainties in the value of E(m) of soot ranging from the low end due to Lee and Tien (1980) to high end due to Köylü and Faeth (1996). A recent experimental study conducted by Krishnan et al. (1999) supported the value of E(m) of soot established previously by Dalzell and Sarofim (1969), Stagg and Charralampopoulos (1993), and Köylü and Faeth (1996). Experimental data of E(m) of soot available in the literature indicate that E(m) is weakly dependent on wavelength in the visible. To our knowledge, no experimental evidence or data on the temperature dependence of E(m) of soot have been published in the open literature. Second, although individual (primary) soot particle can be approximately treated as a sphere as revealed by transmission electron microscopy (TEM) (Megaridis and Dobbins, 1990), soot consists of fractal-structured aggregates and there is usually strong bridging between primary particles (Megaridis and Dobbins, 1990; Faeth and Köylü, 1995). Third, soot contains other elements such as O and H instead of pure carbon and the percentages of these elements in soot vary throughout a flame. Fourth, there seems no experimental data on soot evaporation available in the literature; instead, it is often assumed that soot can be modeled as graphite as far as evaporation is concerned. Thermodynamic equilibrium calculations (Leider et al., 1973) indicate that graphite evaporation releases multi-species including C_1-C_7 and the relative concentrations of these species are temperature and also laser energy dependent (Gaumet et al., 1993). In addition, the nano-scale soot evaporation is a non-equilibrium process. It is also worth noting that there are significant morphological changes for laser-heated soot particles demonstrated by Vander Wal and Choi (1999) and Vander Wal et al. (1995). Incorporation of the morphological changes of laser-heated soot into the LII model is difficult and requires substantial research effort. Lastly, the physical properties of soot at temperatures around 4000 K are subject to significant uncertainties, especially vapor pressure and heat of evaporation. All these factors make the development of sophisticated theoretical LII models extremely difficult. Nevertheless, the theoretical LII model that has been developed in the literature needs to be further improved. The objective of this study is to evaluate the capability and limitations of the current LII model for prediction of excitation curve.

In this study the current LII model was applied to predict the variation of the normalized soot incandescence signal with laser intensity in a well-characterized laminar diffusion flame and the results were compared with the experimental data in the literature. Effects of the spatial and temporal profiles of the pulsed laser were also investigated.

NOMENCLATURE

c	Speed of light in vacuum, 2.9979×10^8 m/s
c_s	Specific heat of soot, J/kg K
C_a	Absorption cross section of soot particle, nm^2
D	Diameter of soot particle, nm
E(m)	Refractive index function for absorption, $=Im((m^2-1)/(m^2+2))$
f	Eucken factor
G	Geometry-dependent heat transfer factor
h	Planck constant, 6.6262×10^{-34} J s
ΔH_v	Heat of vaporization of graphite, J/mole
k	Imaginary part of the refractive index; Boltzmann constant, 1.3806×10^{-23} J/K
k_a	Heat conduction coefficient of air, W/m K
m	Refractive index of soot, =n+ik
M	Mass of soot particle, g
M_v	Molecular weight of soot vapor, g/mole
n	Real part of the refractive index
n_v	Molecular number density of soot vapor, molecules/m^3
N_A	Avogadro's number
N_v	Molecular flux of evaporated carbon, molecules/m^2 s
P_v	Vapor pressure of soot, Pa
q	Laser intensity, W/m^2
q_{rad}	Heat loss term due to radiation, W
Q_a	Absorption efficiency of soot particle
R	Universal gas constant, 8.313 J/mole K
t	Time, s

T	Soot temperature, K
T_g	Gas temperature, K
α	Thermal accommodation coefficient
β	Evaporation coefficient
λ_{MFP}	Mean free path, m
λ	Wavelength, nm
$\gamma(T_g)$	Specific heat ratio
ρ_s	Density of soot, kg/m^3
Γ	Diffusion coefficient of soot vapor, m^2/s

THEORETICAL MODEL

The current theoretical LII model is based on energy and mass conservation of a single primary soot particle of known size. Due to the difficulties of modelling the heat and mass transfer processes of LII mentioned in the introduction, several assumptions have to be introduced in order to formulate the LII model. The key assumptions commonly made in LII models are (1) soot aggregates consist of just-touching monodisperse spherical primary particles and there is no interference between primary particles as far as laser energy absorption and subsequent heat and mass transfer are concerned, (2) the soot primary particle is treated as a spherical graphite particle as far as evaporation process is concerned, (3) the value of E(m) of soot is independent of temperature, and (4) the evaporation rate of soot can be calculated using the thermodynamic equilibrium model for graphite. Limitations of these assumptions have been discussed by Vander Wal and Jensen (1998), Will et al. (1998) among others.

It has been established experimentally that primary particle distributions, unlike aggregate distributions, tend to be near mono-disperse. Köylü and Faeth (1992) found primary particle sizes to be near normally distributed with a standard deviation 17%-25% of the mean for a range of gaseous and liquid fuels. Megaridis and Dobbins (1990) observed near mono-disperse primary particle distributions in a laminar ethylene diffusion flame with the standard deviation varying from 13% to 22% of the mean primary particle size. By contrast the distribution of the number of primary particles per aggregate is much broader and follows a log-normal distribution. Köylü and Faeth (1992) observed aggregate distributions with a geometric standard deviation of 2.9 independent of fuel type. Thus, 63% of the aggregates were in the range $1/2.9< N/N_g <2.9$, where N and N_g are the number and geometric mean of the log-normal distribution of primary particles in an aggregate, respectively. However, there is normally considerable bridging between primary soot particles as revealed by TEM. Therefore, the first assumption is only partially valid. The second and fourth assumptions made above are also in question in view of the morphological changes of soot particles under laser heating. Nevertheless, these assumptions are commonly employed in the LII modelling community (Snelling et al., 1997; Will et al., 1998; McManus et al., 1998; Schraml et al., 2000).

Based on the first assumption, the heat and mass transfer processes of LII of soot aggregates can be modelled by considering a single primary soot particle. It has been pointed out by Melton (1984), Dasch (1984), and Hofeldt (1993) that the temperature gradients inside a primary soot particle in LII experiments can be neglected. The primary soot particles for most flames are below 50 nm. As such they are in the Rayleigh regime for absorption and the Knudsen regime for conduction. The following equations are based on the analysis of Eckbreth (1977) as modified by Melton (1984) and Hofeldt (1993), who used the results of the heat balance equation for a spherical particle, and the analysis of McCoy and Cha (1974) of energy transfer in the transition between continuum and Knudsen regimes. The energy balance equation is

$$C_a q - \frac{2k_a(T-T_g)\pi D^2}{(D+G\lambda_{MFP})} + \frac{\Delta H_v}{M_v}\frac{dM}{dt} + q_{rad} - \frac{1}{6}\pi D^3 \rho_s c_s \frac{dT}{dt} = 0 \qquad (1)$$

The terms in Eq.(1) represent, in order, the laser energy absorption by soot particle, heat conduction loss from the soot particle to the surrounding gas in the transition regime, heat loss due to soot evaporation, heat loss through the mechanism of thermal radiation, and finally the rate of soot particle internal energy change. The mass conservation equation is written as

$$\frac{dM}{dt} = \frac{1}{2}\rho_s \pi D^2 \frac{dD}{dt} = -\pi D^2 N_v \frac{M_v}{N_A} \qquad (2)$$

such that the vapor mass evaporated is equivalent to the particle mass lost.

The absorption cross section of a primary soot particle in the Rayleigh limit is given as

$$C_a = \frac{\pi^2 D^3 E(m)}{\lambda} \qquad (3)$$

where E(m) is a wavelength dependent function of the soot refractive index *m* and is given as

$$E(m) = \frac{6nk}{(n^2-k^2+2)^2 + 4n^2k^2} \qquad (4)$$

The absorption cross section of laser radiation by soot is proportional to the refractive index function, E(m). Thus, it is E(m), and not the refractive index, which must be known to model laser heating of the soot particles. Gravimetric calibration of the dimensionless extinction coefficient for soot produced by burning crude oil (Dobbins, et al. 1994) and acetylene (Choi, et al. 1995) gave almost identical values. Wu et al. (1996) measured both the dimensionless extinction and the soot scattering and were thus able to determine E(m) directly. They found that E(m) was independent of fuel type for a range of gaseous and liquid fuels and was also independent of wavelength over the range 400 nm to 800 nm. Their dimensionless extinction coefficients around 5 were somewhat lower than those of Choi et al. (1995) and Dobbins et al. (1994) who obtained dimensionless extinction coefficients in the range 8-9. In a subsequent detailed study this same group (Krishnan et al., 1999) is now observing dimensionless extinction coefficients in the same range as those of Choi et al. and Dobbins et al., and values of E(m) of 0.3 throughout the visible

wavelength range. This data and that of Dalzell and Sarofim (1969) and Stagg and Charalampopoulos (1993) are in reasonable agreement, all indicating values of E(m) of 0.2 – 0.3 largely independent of wavelength in the visible.

In the heat conduction term, the geometry dependent heat transfer coefficient G is defined as

$$G = \frac{8f}{\alpha(\gamma+1)} \tag{5}$$

where f is the Eucken factor (5/2 for monatomic species), α is the accommodation coefficient (a value of 0.9 is commonly assumed. The molecular flux N_v associated with the soot evaporation in Eq.(2), which is in the transition regime, is given as (Hofeldt, 1993)

$$\frac{1}{N_v} = \frac{1}{N_c} + \frac{1}{N_K} \tag{6}$$

where subscripts c and K refer to the continuum and Knudsen (free molecule) regimes. In the Knudsen regime, the molecular flux N_K is calculated as (Kennard, 1938)

$$N_K = \beta n_v \sqrt{\frac{RT}{2\pi M_v}} \tag{7}$$

The evaporation coefficient β takes a value of about 0.8 in the absence of better knowledge. The molecule number density of soot vapor can be written as, using the ideal gas equation

$$n_v = \frac{P_v N_A}{RT} \tag{8}$$

In the continuum regime, the soot vapor molecular flux N_c can be calculated as (McCoy and Cha, 1974)

$$N_c = 2n_v \frac{\Gamma}{D} \tag{9}$$

Results of the thermodynamic equilibrium calculations of Leider et al. (1973) were employed in the present LII model to obtain the soot vapor molecular weight M_v and vapor pressure P_v. Seven carbon species (C_1-C_7) were considered in the thermodynamic equilibrium calculations of Leider et al. (1973). Their relative concentrations in the soot vapor are temperature dependent. The heat of vaporization of soot (assuming pure graphite) is obtained from the Clausius-Clapeyron equation using the vapor pressure data of Leider et al. (1973) as a function of temperature.

The radiation heat loss term, q_{rad}, which produces the incandescence signal is orders of magnitude smaller than other terms and therefore can be neglected as a heat loss mechanism (Dasch, 1984; Snelling et al., 1997; Will et al., 1998).

The incandescence signal emitted by a single primary soot particle through the mechanism of thermal radiation can be modelled as

$$S_{LII} \propto \frac{2c^2 h}{\lambda^5} \frac{1}{\left(\exp^{\frac{hc}{k\lambda T}} - 1\right)} D^2 \, Q_a(\lambda) \tag{10}$$

The absorption efficiency of soot particle is given as

$$Q_a = \frac{4\pi D}{\lambda} E(m) \tag{11}$$

Combining Eqs.(10) and (11) indicates that the spectral LII signal is proportional to the particle volume, the function E(m), and exponentially dependent on the temperature.

RESULTS AND DISCUSSIONS

The LII model discussed above consists of a set of two coupled differential equations for the soot temperature (the energy conservation equation) and the soot particle diameter (the mass conservation equation). They were solved numerically using a Runge-Kutta integration routine. Once these equations are solved, the LII signal intensity, Eq.(10), is readily obtained.

The LII model was used to predict the experimental excitation curve reported by Ni et al. (1995). A frequency-doubled Nd:YAG pulsed laser (532 nm wavelength) operating at 10 Hz with a pulse width of 7 ns FWHM was used in their experiment. The laser intensity distribution across the laser beam is near-Gaussian. A 1-mm-pinhole placed in front of the flame was introduced in order to produce a uniform spatial laser intensity profile across the laser beam. A co-flow laminar ethene diffusion flame was studied. The primary soot particle size at different flame heights had been reported by Megaridis and Dobbins (1989) using TEM sampling. The LII signal was obtained at a height of 40 mm above the fuel exit and at a radial location where the soot volume fraction peaks. The corresponding primary soot particle diameter is about 32 nm (Megaridis and Dobbins, 1989). The prompt LII signal reported by Ni et al. (1995) was detected at 400 nm wavelength, beginning at the end of the laser pulse for 18 ns.

The temporal profile and total duration of the laser used in the experiment of Ni et al. (1995) were not reported. Therefore, a typical Q-switch laser temporal profile shown in Fig.1 was assumed for the laser used in their experiment and also used in the present calculations. The total duration of this pulsed laser is about 30 ns. Unless otherwise indicated, the soot particle diameter, the laser temporal profile, and the gate width and timing for the collection of the prompt LII signal used in the calculations were 32 nm, Q-switched, and 18 ns and beginning at 30 ns, respectively.

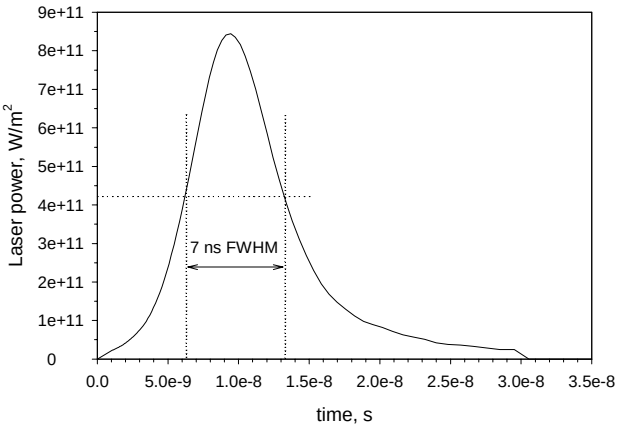

Fig.1 Temporal distribution of the laser intensity

Effects of the detector gate width and timing

Figure 2 displays the predicted excitation curves and the experimental curve of Ni et al. (1995) for a uniform laser intensity profile and using the soot refractive index of Dalzell and Sarofim (1969). The value of E(m) at 532 nm based on the refractive index of Dalzell and Sarofim is 0.261. Calculations were carried out for the laser fluence dependence of three prompt LII signals with different gate widths and/or timing as indicated in the figure. The purpose of performing these three LII signal calculations is to investigate the effects of these two parameters (gate width and timing) on the excitation curve.

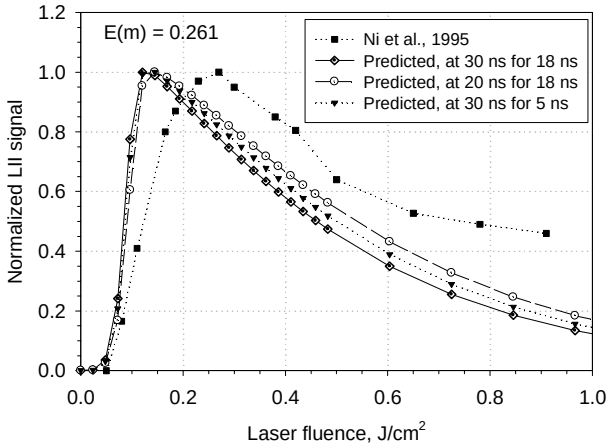

Fig.2 Comparison between the predicted and the experimental excitation curves for a rectangular laser beam.

A common feature of the curves shown in Fig.2 is that the LII signal rises rapidly with increasing laser fluence to reach a maximum then decreases gradually at higher fluences. Hereafter the laser fluence at which the excitation curve peaks is referred to as the *threshold laser fluence*. The shape of the three predicted excitation curves is similar to the experimental curve of Ni et al. (1995). However, the threshold laser fluences of the predicted curves are about a factor of 2 lower than the threshold value (about 0.27 J/cm^2) found experimentally by Ni et al. In addition to the discrepancy in the value of the threshold laser fluence, the trend of the curve at laser fluences higher than about 0.65 J/cm^2 is also different. The modelled curves continue to decrease at a much higher rate than the experimental curve with increasing laser fluence. The experimental curve, however, actually shows only slight reduction in LII signal at laser fluences above 0.65 J/cm^2. It is very likely that at these relatively high laser fluences the detected LII signal consists of contributions from both thermal radiation and the emissions from the C_2 swan bands at 400 nm, whereas modelled signal is purely based on thermal radiation. Figure 2 also shows that the effects of the gate width and timing for collecting the prompt LII signal on the excitation curve are relatively weak. Therefore, the discrepancy in the threshold laser fluences between the modelled and the experimental curves cannot be attributed to the uncertainties in the timing or gate width for the collection of the prompt LII signal.

Effects of the initial soot particle size

The potential effect of the initial soot particle size on the excitation curve was investigated by considering three initial sizes, 22, 32, and 42 nm and the results are shown in Fig.3. The value of E(m) based on the refractive index of Dalzell and Sarofim was employed in these calculations. These results indicate that the excitation curve is very insensitive to the initial soot particle size. This conclusion is valid for particle sizes greater than about 10 nm.

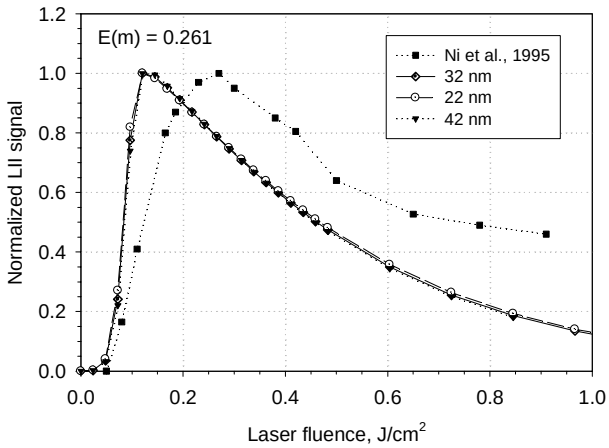

Fig.3 Effect of the initial soot particle size on the prediction of the excitation curve.

Effects of the value of E(m)

The uncertainty in the prediction of the excitation curve due to the uncertainty in the value of E(m) was investigated by calculating the excitation curve using two values of E(m), one is the high value due to Dalzell and Sarofim, and the other is the low value due to Lee and Tien (1981) (0.176 at 532 nm). The predicted excitation curves using these two values of E(m) are compared with the experimental curve of Ni et al. (1995) in Fig.4. It can be seen that the excitation curve based on the E(m) of Lee and Tien is in better overall agreement with the experimental curve than that based on the E(m) of Dalzell and Sarofim. This is attributed to the fact that the E(m) value of Lee and Tien is smaller than that of Dalzell and Sarofim. Therefore, use of E(m) of Lee and Tien results in a delayed rise of the prompt LII signal with the laser fluence, resulting in better agreement for the threshold laser fluence with the experiment of Ni et al. (1995). Actually the excitation curve predicted using the E(m) of Lee and Tien can be obtained from the curve based on the E(m) of Dalzell and Sarofim by simply multiplying the laser fluences by 0.261/0.176, since the laser absorption term is proportional to E(m)q, Eqs.(1) and (3). Fig.4 suggests that the value of E(m) of Lee and Tien is a better choice as far as the excitation curve prediction using the present LII model is

concerned. Fig.4 also shows that the E(m) of Lee and Tien predicts a much slower rise of the LII signal at laser fluence lower than about 0.125 J/cm^2 and a faster rise at higher laser fluences leading to a smaller value of the threshold laser fluence than the experimental one. Based on the linear dependence of the laser absorption term on E(m), this figure implies that it is not possible to reproduce the experimental excitation curve by simply adjusting the constant value of E(m). Assuming that the present evaporation model is acceptable, Fig.4 suggests that E(m) is a function of temperature rather than a constant. Further research and experimental evidence are required to support this suggestion.

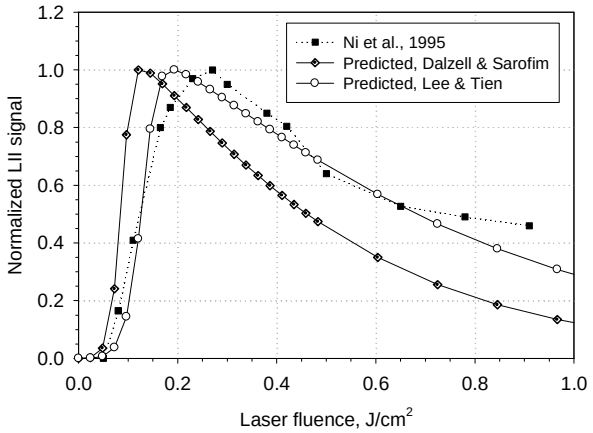

Fig.4 Effect of E(m) on the predicted of the excitation curve.

Another explanation for the discrepancy in the threshold laser fluence is the incorrect treatment of the evaporation rate of soot at high laser fluences. The present model leads to overprediction of soot evaporation and therefore a smaller soot particle at the end of the laser pulse. This potentially severe drawback of the present LII model has also been noticed by Wainner and Seitzman (1999). It is worth pointing out that the most important processes in determining the excitation curve of the prompt LII signal are laser energy absorption by the soot particle and the heat loss through soot evaporation mechanism. Heat conduction plays an important role only at low laser fluences or after the soot particle cools down below the evaporation temperature. Therefore, the present evaluation study of the LII model concerns the adequacy of the laser absorption and the evaporation terms of the energy conservation equation. The discrepancies between the predicted excitation curve using the E(m) of Dalzell and Sarofim and the experimental curve in the slope of rise and the threshold laser fluence may be entirely caused by the incorrect treatment of the evaporation term, which is likely given the fact that the present LII model does not incorporate the morphological changes of laser-heated soot observed by Vander Wal and co-workers (1995; 1999). It is more likely that both the uncertainty of E(m) at very high temperatures (above 3000 K) and the incorrect treatment of the evaporation term are responsible for these discrepancies. However, their effects cannot be quantified in the present study.

Effects of the spatial laser intensity distribution

Effects of the laser intensity distribution across the laser beam were studied by calculating the normalized prompt LII signals for four different profiles described by

$$q = \exp(-\frac{2x^p}{\sigma^2}) \qquad (12)$$

where σ=1 and different distributions of laser intensity across the laser beam are achieved by varying the value of p. The four profiles considered are shown in Fig.5 for p = 2 (Gaussian), 6, 16 and ∞ (uniform).

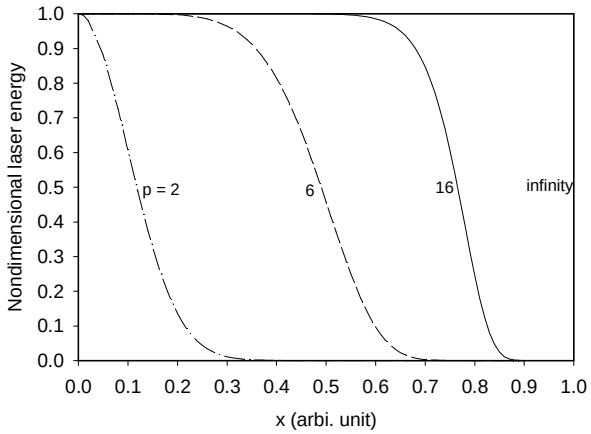

Fig.5 Four spatial laser intensity distributions considered in the calculations.

The corresponding theoretical excitation curves based on the E(m) of Lee and Tien are compared with the experimental curve of Ni et al. (1995) in Fig.6. For non-uniform laser intensity profiles, the profiles can be viewed as containing a number of uniform laser beams of width Δx. Summation of the contribution of each uniform laser of width Δx yields the LII signal generated by the non-uniform laser. These results indicate that the excitation curve is strongly dependent on the spatial laser intensity distribution. Experimentally the strong effect of the spatial laser intensity distribution on the excitation has been observed by Ni et al. (1995). A similar finding has also been demonstrated theoretically by Tait and Greenhalgh (1992, 1993) for rectangular and Gaussian laser beams. The physical reason behind this strong dependence has been discussed by Shaddix and Smyth (1996) and Snelling et al. (1997).

Figure 7 compares the predicted and the experimental excitation curves for the Gaussian laser beam. The dependence of the normalized LII signal on the mean laser fluence was displayed in this figure. Since Ni et al. (1995) did not report how the mean laser fluence was defined in their experiment, the mean laser fluence was assumed to be e^{-1} of the peak laser fluence in the comparison. Reasonably good agreement between

the prediction and experimental results can be observed, although the rate of rise leading to the threshold is still greater for the theory over the experiment.

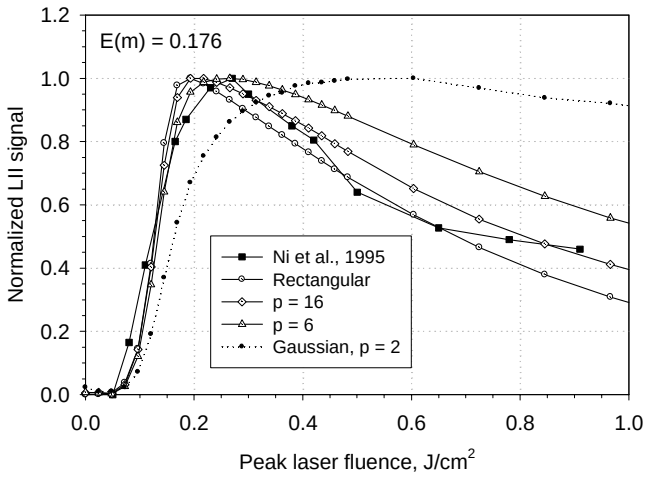

Fig.6 Effects of the spatial laser intensity distribution on the prediction of the excitation curve.

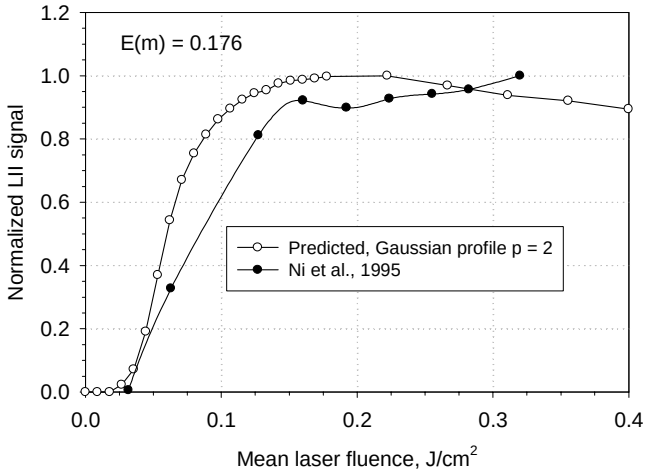

Fig.7 Comparison between the predicted and the experimental excitation curves for a Gaussian laser intensity distribution.

Effects of the temporal laser intensity distribution

To investigate the effects of the temporal laser intensity distribution, three temporal profiles were considered as shown in Fig.8 for identical laser fluence of 0.725 J/cm^2. The spatial distribution of these three cases is uniform. Excitation curves of these three cases were calculated for the prompt LII signal collected at the end of each laser pulse for 18 ns and the results are compared in Fig.9. These results show that the excitation curve is insensitive to the temporal distribution of the laser intensity as long as the laser energy is delivered sufficiently rapidly. These results support the suggestion of Shaddix and Smyth (1996) to use laser fluence (J/cm^2) in the study of the laser power dependence of LII signal instead of laser intensity (W/cm^2).

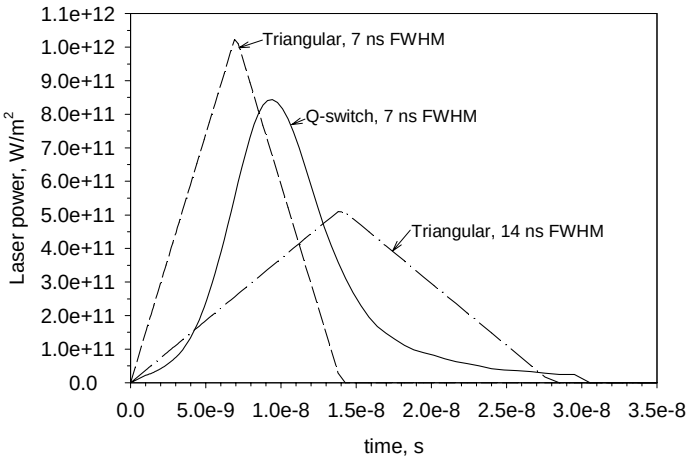

Fig.8 Temporal distributions of laser intensity investigated in the calculations.

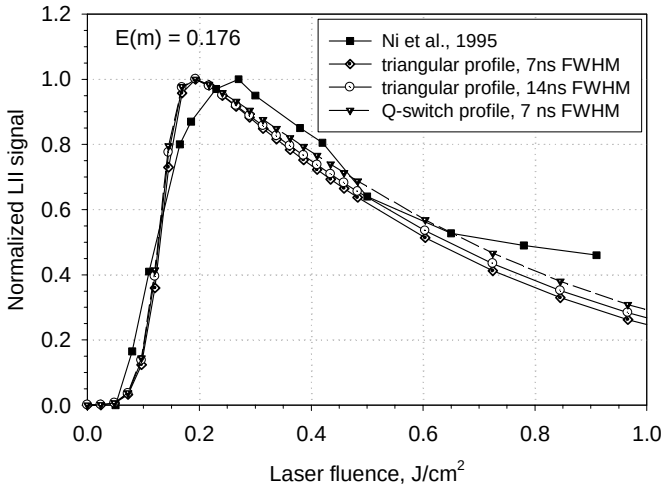

Fig.9 Effects of the temporal distribution of the laser intensity on the prediction of the excitation curve.

Although the temporal distribution of the laser intensity has only a slight effect on the excitation curve, it has significant impact on the history of the predicted soot temperature and diameter as shown in Fig.10. For a given total laser energy, the shorter the laser pulse, the faster the temperature rise and the higher the peak soot temperature, Fig.10(a). Correspondingly, the shorter the laser pulse, the smaller the soot particle size after the laser pulse, Fig.10(b). It is therefore important to report the temporal distribution of laser intensity for the pulsed laser used in LII experiments.

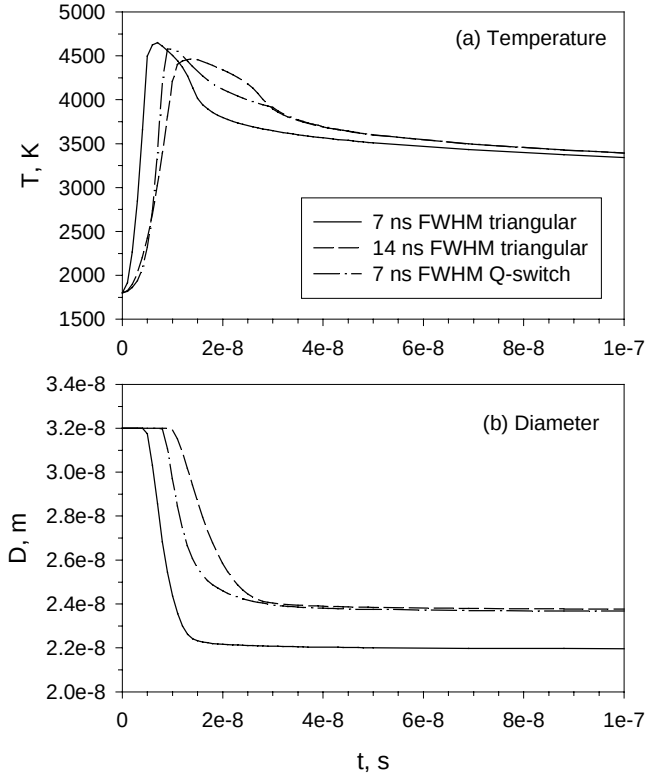

Fig.10 Effects of the temporal distribution of the laser intensity on the predicted history of soot particle temperature and diameter using E(m) = 0.176.

CONCLUSIONS

The current theoretical LII model was applied to predict the laser fluence dependence of the prompt LII signal in a laminar ethylene flame with known primary soot particle size. The model successfully reproduces the overall trend of the experimental excitation curve obtained using a spatially uniform pulsed laser: a rapid rise, rounded peak followed by gradual tail-off at higher laser fluences. However, the model fails to predict the correct threshold laser fluence and the trend of the curve at high fluences (>0.6 J/cm^2). The failure of the current LII model may be attributed to: (1) the uncertainty of E(m) and its dependence on temperature and (2) the incorrect treatment of the evaporation rate at high laser fluences. Use of the value of E(m) established by Lee and Tien yields better overall agreement between the predicted excitation curve by the present LII model and the experimental curve of Ni et al. Further theoretical and experimental research are required to establish a more reliable value of E(m) for soot at temperatures comparable to LII.

Further improvement of the current LII model should also take into account the following facts: (1) primary soot particles are in general connected with each other with significant bridging, and (2) laser-heated soot particles experience considerable morphological changes.

It was also found that the spatial distribution of the laser intensity across the laser beam has a much stronger effect on the excitation curve than the temporal distribution. In addition, the predicted excitation curve is insensitive to the initial soot particle size and the detector gate width and timing. The temporal distribution of the laser intensity, however, affects significantly the evolution history of the soot temperature and diameter. It is recommended that both the spatial and temporal distributions of the laser intensity of the pulsed laser used in LII experiments should be reported.

ACKNOWLEDGMENTS

Partial funding for this study has been provided by the Canadian Government PERD Program's Particulates Initiatives.

REFERENCES

Choi, M. Y., Mulholland, G. W., Hamins, A., and Kashiwagi, T., 1995, "Comparisons of the Soot Volume Fraction Using Gravimetric and Light Extinction Techniques," Combustion and Flame, Vol.102, pp.161-169.

Dalzell, W. H., and Sarofim, A. F., 1969, "Optical Constants of Soot and Their Application to Heat-Flux Calculations," Journal of Heat Transfer, Vol. 91, pp. 100-104.

Dasch, C. J., 1984, "Continuous-Wave Probe Laser Investigation of Laser Vaporization of Small Soot Particles in a Flame," Applied Optics, Vol.23, No.13, 2209-2215.

Dobbins, R. A., Mulholland, G. W., and Bryner, N. P., 1994, "Comparison of a Fractal Smoke Optics Model with Light Extinction Measurements," Atmos. Environ. Vol.28, no.5, pp.889-97.

Eckbreth, A. C., 1977, "Effects of Laser-Modulated Particulate Incandescence on Raman Scattering Diagnostics," Journal of Applied Physics, Vol. 48, No. 11, pp. 4473-4479.

Faeth, G. M. and Köylü, Ü. Ö., 1995, "Soot Morphology and Optical Properties in Nonpremixed Turbulent Flame Environments," Combustion Science and Technology, Vol. 108, pp. 207-229.

Gaumet, J. J., Waklsaka, A., Shimizu, Y., and Tamori, Y., 1993, "Energetics for Carbon Clusters Produced Directly by Laser Vaporization of Graphite: Dependence on Laser Power and Wavelength," J. Chem. Soc. Faraday Trans., Vol.89, no.11, pp.1667-1670.

Hofeldt, D. L., 1993, "Real-Time Soot Concentration Measurement Technique for Engine Exhaust Streams," SAE paper 930079.

Kennard, E. H.,1938, Kinetic Theory of Gases, McGraw-Hill Book Companym New York, p.63, 69.

Köylü, Ü. Ö., and Faeth, G. M., 1992, "Structure of Overfire Soot in Buoyant Turbulent Diffusion Flames at Long Residence Times," Combustion and Flame, Vol.89, no.2, pp.140-156.

Köylü, Ü. Ö., and Faeth, G. M., 1996, "Spectral Extinction Coefficient of Soot Aggregates from Turnulent Diffusion Flames," ASME Journal of Heat Transfer, Vol.118, pp.415-421.

Krishnan, S. S., Lin, K. C., and Faeth, G. M., 1999, "Optical Properties in the Visible of Overfire Soot in Large Buoyant Turbulent Diffusion Flames," Submitted to ASME Journal of Heat Transfer.

Lee, S. C., and Tien, C. L., 1981, "Optical Constants of Soot in Hydrocarbon Flames," Eighteen Symposium (International) on Combustion, The Combustion Institute, pp. 1159-1166.

Leider, H. R., Krikorian, O. H., and Young, D. A., 1973, "Thermodynamic Properties of Carbon up to the Critical Point," Carbon, Vol.11, pp.555-563.

McCoy, B. J. and Cha, C. Y., 1974, "Transport Phenomena in the Rarefied Gas Transition Regime," Chemical Engineering Science, Vol. 29, pp.381-388.

McManus, K. R., Frank, J. H., Allen, M. G., 1998, and Rawlins, W. T., "Characterization of Laser-Heated Soot Particles Using Optical Pyrometry," AIAA 98-0159, 36th Aerospace Sciences Meeting and Exhibit, Reno, NV.

Megaridis, C. M. and Dobbins, R. A., 1989, "Comparison of Soot Growth and Oxidation in Smoking and Non-Smoking Ethylene Diffusion Flames," Combust. Sci. Tech., Vol. 66, 1-16.

Megaridis, C. M. and Dobbins, R. A., 1990, "Morphological Description of Flame-Generated Materials," Combustion Science and Technology, Vol.71, pp.95-109.

Melton, L. A., 1984, "Soot Diagnostics Based on Laser Heating," Applied Optics, Vol. 23, No. 13, pp.2201-2208.

Ni, T., Pinson, J. A., Gupta, S., and Santoro, R. J., 1995, "Two-Dimensional Imaging of Soot Volume Fraction by the Use of Laser-Induced Incandescence," Applied Optics, Vol.34, No.30, pp. 7083-7091.

Schraml, S., Dankers, S., Bader, K., Will, S., and Leipertz. A., 2000, "Soot Temperature Measurements and Implications for Time-Resolved Laser-Induced Incandescence (TIRE-LII)," Combustion and Flame, Vol.120, pp.439-450.

Snelling, D. R., Smallwood, G. J., Campbell, I. G., Medlock. J. E., and Gülder, Ö. L., 1997, "Development and Application of Laser-Induced Incandescence by Comparison with Excitation Measurements in Laminar Premixed, Flat Flames," AGARD 90th Symposium of the Propulsion and Energetics Panel on Advanced Non-intrusive Instrumentation for Propulsion Engines, Brussels, Belgium.

Stagg, B. J. and Charalampopoulos, T. T., 1993, "Refractive Indices of Pyrolytic Graphite, Amorphous Carbon, and Flame Soot in the Temperature range 25 Degree to 600 Degree C," Combustion and Flame, Vol.94, no.4, pp. 381-396.

Tait, N. P. and Greenhalgh, D. A., 1992, "2D laser induced fluorescence imaging of parent fuel fraction in nonpremixed combustion," 24th Symp. (Int.) on Combustion, pp.1621-1628, The Combustion Institute.

Tait, N. P., and Greenhalgh, D. A., 1993, "PLIF Imaging of Fuel Fraction in Practical Devices and LII Imaging of Soot," Ber. Bunsenges. Phys. Chem., Vol. 97, No.12, pp.1619-1625.

Will, S., Schraml, S., Bader, K., and Leipertz, A., 1998, "Performance Characteristics of Soot Primary Particle Size Measurements by Time-Resolved Laser-Induced Incandescence," Applied Optics, Vol.37, No.24, pp.5647-5658.

Vander Wal, R. L., and Weiland, K. J., 1994, "Laser-Induced Incandescence: Development and Characterization towards a Measurement of Soot-Volume Fraction," Applied Physics B 59, pp. 445-452.

Vander Wal, R. L., Choi, M. Y., and Lee, K.-O., 1995, "The Effects of Rapid Heating of Soot: Implications When Using Laser-Induced Incandescence for Soot Diagnostics," Combustion and Flame, Vol.102, pp.200-204.

Vander Wal, R. L., and Jensen, K. A., 1998, "Laser-Induced Incandescence: Excitation Intensity," Applied Optics, Vol. 37, No. 9, pp.1607-1616.

Vander Wal, R. L., and Choi, M. Y., 1999, "Pulsed Laser Heating of Soot: Morphological Changes," Carbon, Vol.37, pp.231-239.

Wu, J. S., Krishnan, S. K., and Faeth, G. M., 1996. "Refractive Indices at Visible Wavelengths of Soot Emitted from Buoyant Turbulent Diffusion Flames," Proceedings of the 31st ASME National Heat Transfer Conference., Houston, TX, USA, American Society of Mechanical Engineers, Heat Transfer Division, (Publication) HTD.